NJC

Accepted Manuscript

Journal Name

Dynamic Article Links▶

ARTICLE TYPE

Spruce branched α-Fe₂O₃ nanostructures as potential scaffold for highly-sensitive and selective glucose biosensor

Ahmad Umar,*,[a,b,†] **Rafiq Ahmad,**[c,†] **Ali Al-Hajry,**[a] **Sang Hoon Kim,**[a] **Mohamed Eisa Abaker,**[a] **and Yoon-Bong Hahn**[c]

This paper presents the fabrication of highly sensitive and selective glucose biosensor based on spruce branched α-Fe₂O₃ nanostructures. The spruce branched α-Fe₂O₃ nanostructures were synthesized by hydrothermal process and characterized by using various techniques. The fabricated glucose biosensor
10 exhibited a very-high and reproducible sensitivity of 85.384 µAmM^{-1}cm^{-2} with a response time less than 2 sec and detection limit (based on S/N ratio) of 1µM. A linear dynamic range from 0.003 ~ 33 mM with correlation coefficient (R^2) of 0.9996 were observed for the fabricated biosensor.

1. Introduction

The concentration of glucose in blood is a crucial parameter for
15 the diabetes diagnosis and treatment.[1] With more than 220 million people affected, diabetes has become one of the major health issues worldwide, and the number of diabetes patients is expected to double in 20 years.[2] Hence, it is of significant importance to develop innovative and new approaches for
20 glucose detection. Various methods have been used to develop biosensors for continuous glucose monitoring such as electrochemical methods, colorimetry, conductometry, optical methods and fluorescent spectroscopy.[3-10] Among them, the amperometric enzyme electrodes, based on glucose oxidase
25 (GOx), have played a leading role for the determination of glucose due to their high sensitivity, repeatability and simple operation. Enzyme based electrochemical biosensors are extensively studied as it can provide convenient, rapid and highly specific measurements. Such enzyme based glucose biosensors
30 have been developed and used in medical, environmental, food, and military applications. Since the development of the first glucose biosensor, improvement of the response performance of enzyme electrodes has been the main focus of biosensor research.[11]
35 Different methods have been suggested to get optimized sensing performances that not only include various enzyme immobilization techniques i.e. electrostatic binding, embedding and covalent binding but also use of mediators like Prussian Blue.[12-18] Among them, mostly electrostatic binding have been
40 used to immobilize enzymes due to its comparable simplicity.[19,20] In this regard significant research efforts have been generated to utilize the metal-oxide matrices for bio-sensing application and a number of matrices based on TiO₂, ZnO, SnO₂, ZrO₂ and CeO₂ have been exploited.[21-29] Among the various nanomaterials,
45 Nanoparticles of various ferric oxides (hematite, magnetite, amorphous Fe₂O₃, β-Fe₂O₃ and ferrihydrite) incorporated into

carbon paste have exhibited electrocatalytic properties towards hydrogen peroxide reduction.[30] Kaushik*et al.* has fabricated a new glucose biosensor and a urea sensor based on iron oxide
50 nanoparticles-chitosan nanocomposite.[31] Wang *et al.* have developed a novel amperometric glucose biosensor by immobilizing ferritin antibody on the surface of Fe₃O₄ nanoparticles (Fe₃O₄ NPs)/chitosan (Cs) composite film modified glassy carbon electrode (GCE) for determination of ferritin.[32]
55 In this paper, we are reporting a highly-sensitive and selective glucose biosensor based on spruce branched α-Fe₂O₃ nanostructures. The fabricated sensor showed a very-high and reproducible sensitivity of 85.384 µAmM^{-1}cm^{-2} with the detection limit of 1 µM. Moreover, to the best of our knowledge, this is the
60 first time such high sensitivity and low-detection limit has been achieved for glucose biosensors by using α-Fe₂O₃ nanostructures modified electrodes.

2. Experimental details

2.1. Reagents

65 Potassium hexacyanoferrate(III) [K₃Fe(CN)₆; ≥99.0%], glucose (d-(+)-99.5 %), butylcarbitol acetate (≥99.2%), Nafion (5 wt% in lower aliphatic alcohol and water mixture), uric acid, dopamine, ascorbic acid, cholesterol (water soluble), sodium phosphate monobasic anhydrous (NaH₂PO₄), sodium phosphate dibasic
70 dihydrate (Na₂HPO₄·2H₂O), and sodium chloride (NaCl) and human blood serum (H4522) were purchased from Sigma-Aldrich. Phosphate buffer saline solution (PBS; 0.1 M, pH 7.0) was freshly prepared by mixing solutions of NaH₂PO₄, Na₂HPO₄·2H₂O and NaCl (0.9%) in deionized water prior to the
75 experiments.

2.2. Synthesis of spruce branched α-Fe₂O₃ nanostructures and characterization

The spruce branched α-Fe₂O₃ nanostructures were synthesized by facile hydrothermal process. For the synthesis, in a typical

reaction process, 0.3 g K$_3$[Fe(CN)$_6$] was dissolved in 80 mL of de-ionized water under continuous stirring. Consequently, after stirring, the resultant solution was loaded into a Teflon-lined stainless steel autoclave, sealed it and heated up to 140 °C for 5h.

After completing the reaction, the autoclave was naturally cooled at room-temperature and finally brown product was obtained which was washed with DI water and ethanol sequentially and dried at 60 °C for 2h. The synthesized products were examined in terms of their morphological, structural, compositional and biosensing properties.

The general morphologies of as-synthesized spruce branched α-Fe$_2$O$_3$ nanostructures were examined by FESEM (JEOL-JSM-7600F) attached with energy dispersive spectroscopy (EDS) and transmission electron microscopy (TEM; JEOL-JEM-2100F) equipped with high-resolution TEM (HRTEM). The crystallinity and crystal phases were characterized by X-ray diffraction (XRD; PAN analytical Xpert Pro.) pattern measured with Cu-Kα Radiation (λ=1.54178 Å) in the range of 10-70º. The chemical composition of as-synthesized spruce branched α-Fe$_2$O$_3$ nanostructures was examined by Fourier transform infrared (FTIR; Perkin Elmer-FTIR Spectrum-100) spectroscopy in the range of 450-4000 cm^{-1}. The scattering properties of as-synthesized α-Fe$_2$O$_3$ nanostructures were examined by Raman-scattering spectroscopy.

2.3. Fabrication of glucose biosensor and measurement

To fabricate the glucose biosensors (Fig. 1), the as-synthesized spruce branched α-Fe$_2$O$_3$ nanostructures were mixed with conducting binders (butylcarbitol acetate) in a weight ratio of 70:30 and the prepared slurry was then cast on silver (Ag) electrode with the area of 4.0 mm^2 (i-ii). Prior to the modification, the silver electrode was polished with the 0.05 µm alumina slurry and then sonicated in DI water. Then, the GOx (1.0 mg/mL) prepared in phosphate buffer (PBS, pH 7.0) was immobilized onto the spruce branched α-Fe$_2$O$_3$ nanostructures by physical adsorption method (iii). The modified electrode was kept overnight for GOx immobilization and subsequently washed to remove un-immobilized enzyme with buffer solution, and dried in nitrogen environment. After drying the modified GOx/α-Fe$_2$O$_3$/Ag electrode, a 5 µl Nafion (0.5 wt%) solution was dropped onto the electrode and dried to form a net-like film on the modified electrode (iv). This step is important; as it protects spruce branched α-Fe$_2$O$_3$ nanostructures and GOx on the surfaces of the modified electrodes. When, not in use, the α-Fe$_2$O$_3$ nanostructures modified Ag electrodes (i.e., Nafion/GOx/α-Fe$_2$O$_3$/Ag electrodes) were stored in PBS at 4.0 °C. The electrochemical experiments were carried out at room temperature using an electrochemical analyzer with a conventional three-electrode configuration: a working electrode (Nafion/GOx/α-Fe$_2$O$_3$/Ag electrodes), a Pt wire as a counter electrode, and Ag/AgCl (sat. KCl) as a reference electrode.

3. Results and discussion

The spruce branched α-Fe$_2$O$_3$ nanostructures were synthesized by facile hydrothermal process and characterized in detail using several techniques. Further, the prepared spruce branched α-Fe$_2$O$_3$ nanostructures were used as supporting matrixes to fabricate enzymatic glucose biosensor. Fig. 1 exhibits the typical
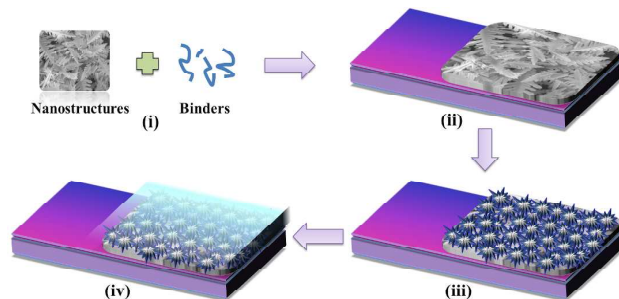
Fig. 1 Schematic illustration of glucose biosensor fabrication process (i) α-Fe$_2$O$_3$ nanostructures mixed with butylcarbitol acetate; (ii) Casting of prepared slurry on Ag electrode; (iii) GOx enzyme immobilization and (iv) Nafion covering.

schematic of glucose biosensor fabrication process in which firstly, slurry of as-synthesized spruce branched α-Fe$_2$O$_3$ nanostructures was made by mixing it with butyl carbitol acetate (i). Further, the prepared slurry was casting on the Ag electrode (ii), which was then immobilized with GOx enzyme (iii) and finally covered with Nafion solution (iv).

3.1. Structural property

The spruce branched structures were synthesized in large quantity as was observed by low-magnification FESEM image shown in Fig. 2(a). The FESEM image clearly reveals that the synthesized spruce branches possess a central trunk with ordered parallel branches distributed both sides of the trunk. The average length of central trunk is ~6±2 µm while the lengths of the branches are ~1.5 ± 1 µm (Fig. 2(b)). The TEM investigation of as-synthesized spruce branch is well-consistent with the observed FESEM results in terms of morphologies and dimensionalities (Fig. 2(c)). The HRTEM image of as-synthesized spruce branched α-Fe$_2$O$_3$ nanostructures exhibited well-defined lattice fringes, which are separated by 0.266, indexed as (014) plane of the rhombohedral α-Fe$_2$O$_3$ structure (Fig. 2(d)). The well-defined and clear lattice fringes of as-synthesized spruce branched α-Fe$_2$O$_3$ nanostructures clearly confirm the purity and well-crystallinity of the synthesized material. The elemental composition of as-synthesized spruce branched α-Fe$_2$O$_3$ nanostructures was examined by EDS attached with FESEM and shown in Fig. 3(a).
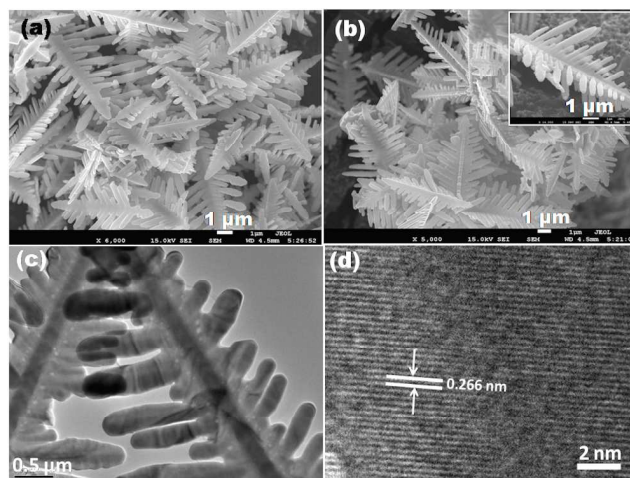
Fig. 2 (a) Low- and (b) high-magnification FESEM images, (c) TEM image and (d) high-resolution TEM image of as-synthesized spruce branched α-Fe$_2$O$_3$ nanostructures.

The observed spectrum confirmed that the spruce branched α-Fe_2O_3 nanostructures are made of iron and oxygen and hence confirms the purity of as-synthesized nanostructures. Fig. 3(b) exhibits the typical XRD pattern of as-synthesized spruce
5 branched α-Fe_2O_3 nanostructures which confirmed that all the reflections in the observed pattern are well matched with the rhombohedral α-Fe_2O_3 structures with calculated lattice constants of a= 5.0356 Å and c= 13.7489 Å. The observed XRD pattern is well matched with the reported literature and JCPDS card no. 33-
10 0664. Because of sharp and strong reflections, it is clear that the synthesized nanomaterials are well-crystalline.

The chemical composition and quality of as-synthesized spruce branched α-Fe_2O_3 nanostructures was examined by the FTIR, in the range of 450-4000 cm^{-1} and shown in Fig. 3(c). The observed
15 spectrum exhibited several well-defined absorption bands at 467, 533, 1381, 1623 and 3441 cm^{-1}. The appearance of two absorption bands at ~467 and ~533 cm^{-1} are due to iron-oxygen (Fe-O) bonds which confirmed the formation of iron oxide.[33] It is reported that a weak absorption band usually appears at 1370-
20 1390 cm^{-1} in the spectrum when the FTIR samples are measured in the air.[33] The presence of weak and a broad absorption bands at 1623 and 3441 cm^{-1} in the spectrum are due to the bending vibration of absorbed water and surface hydroxyl, and O-H stretching mode, respectively.[33] Importantly, except Fe-O, no
25 other significant absorption peak was seen in the spectrum that confirmed that the synthesized nanostructures are pure iron oxide without any significant impurity.

The purity and scattering properties of as-synthesized spruce branched α-Fe_2O_3 nanostructures was examined by Raman-
30 scattering spectroscopy and results are shown in Fig. 3 (d). The hematite, α-Fe_2O_3, belongs to D^6_{3d} crystal space group and according to the group theory; this group of material possesses even phonon lines in the Raman spectrum.[34] The observed Raman-scattering spectrum of as-synthesized spruce branched α-
35 Fe_2O_3 nanostructures exhibited several well-defined peaks at 224, 242, 285, 406, 494, 606, and 1309 cm^{-1} which are similar to the pure α-Fe_2O_3 as reported in the literature.[34] The origination of peaks appeared at 224 and 606 cm^{-1} are related with the Raman-active optical phonons and assigned as Raman-active $A_{1g}(1)$ and
40 $A_{1g}(2)$ modes, respectively. The origination of other well-defined
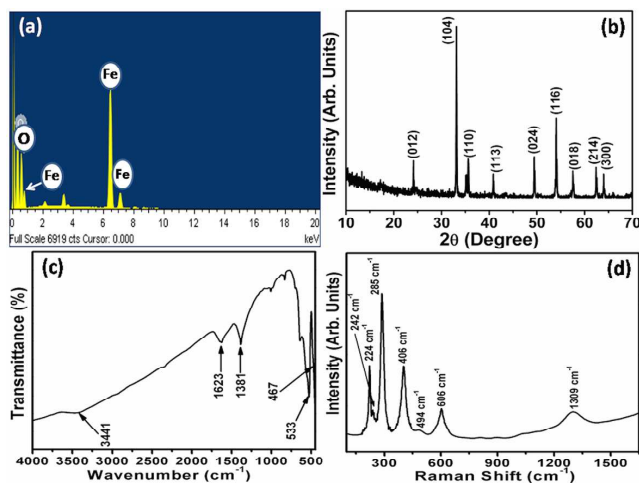
Fig. 3 Typical (a) EDS spectrum, (b) XRD pattern, (c) FTIR spectrum and (d) Raman-scattering spectrum of as-synthesized spruce branched α-Fe_2O_3 nanostructures.
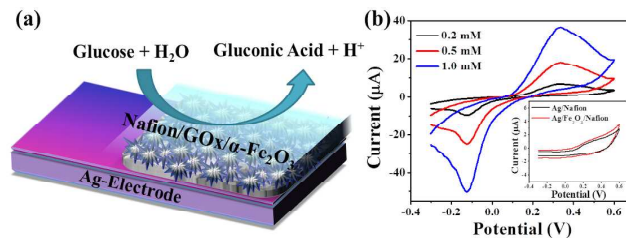
45 **Fig. 4**(a) Schematic of modified silver electrode detecting glucose; (b) CV of Ag/α-Fe_2O_3/GOx/Nafion electrodes in the presence of 0.2, 0.5 and 1.0 mM glucose in 0.1 M PBS (pH 7.0) at scan rate of 100 mV/s. The insert of b is showing CV response of Ag/Nafion and Ag/α-Fe_2O_3/Nafion
50 electrode in 0.2 mM glucose.

peak sat 285, 406, and 494 cm^{-1} are related with Raman-active E_g modes. The presence of a small and suppressed peak at 1309 cm^{-1} is related with the second harmonic vibration mode.

3.2. Electrochemical studies of Ag/α-Fe_2O_3/GOx/Nafion
55 **electrode**

Fig. 4(a) exhibits the schematic of the modification of silver electrode with spruce branched α-Fe_2O_3 nanostructures, GOx and Nafion for efficient detection of glucose. The chemical reactions for enzymatic breakdown of glucose *via* GOx along with the
60 subsequent oxidation of hydrogen peroxide (H_2O_2) are as follows.[35]

$$\text{Glucose} + GO_x(OX) \rightharpoonup \text{Gluconolactone} + GO_x(R) \qquad (1)$$
$$GO_x(R) + O_2 \rightharpoonup GO_x(OX) + H_2O_2 \qquad (2)$$
$$H_2O_2 \rightharpoonup O_2 + 2H^+ + 2e^- \qquad (3)$$
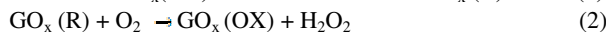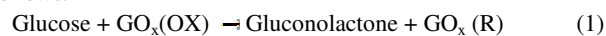
65 Where, GOx converts glucose into gluconolactone, while GOx(OX) is changed into the reduced form GOx(R). The consumed GOx(OX) could be regenerated from GOx(R) through its reaction with the oxygen present in solution. However, the low oxygen dissolved in solution may also lead to the lower sensor
70 response. To avoid this we performed experiments in open at room temperature with an air-saturated solution (oxygen concentration 0.2-0.4 mM) under continuous stirring. The electro-oxidation current of generated H_2O_2, is amperometrically measured on the surface of modified working electrode by the
75 application of suitable redox potential to the platinum electrode, relative to the Ag/AgCl reference electrode. This relates the dependence of current on glucose concentrations. In the present case dissolved oxygen works as mediator and use of mediator like Prussian Blue is not required, which works fine for the oxidation
80 of peroxide. Hence, modified electrodes can be used for quantitatively detection of glucose.

To avoid the electro-formation of a multilayer of Ag_2O, which may further give an anodic current peak, the cyclic voltammetry (CV) were performed in 0.1 M PBS (pH 7.0). Fig. 4(b) shows the
85 CV responses in the potential range of -0.3 to +0.6 V for Ag/Nafion and Ag/α-Fe_2O_3/Nafion electrode (inset) in the presence of 0.2 mM glucose and Ag/α-Fe_2O_3/GOx/Nafion electrodes in the presence of 0.2, 0.5 and 1.0mM glucose. No peak has been observed in CV curves for Ag/Nafion (black-line)
90 and Ag/α-Fe_2O_3/Nafion electrodes (red-line), which is ascribed to the high quality and high stability of sputtered Ag layer. However, a dramatic change in the CV curves were seen by the Ag/α-Fe_2O_3/GOx/Nafion electrode with a clear and defined redox peaks appeared at +0.33 V (oxidation) and -0.12 V (reduction)
95 are due to the H_2O_2 generation during the oxidation of glucose by
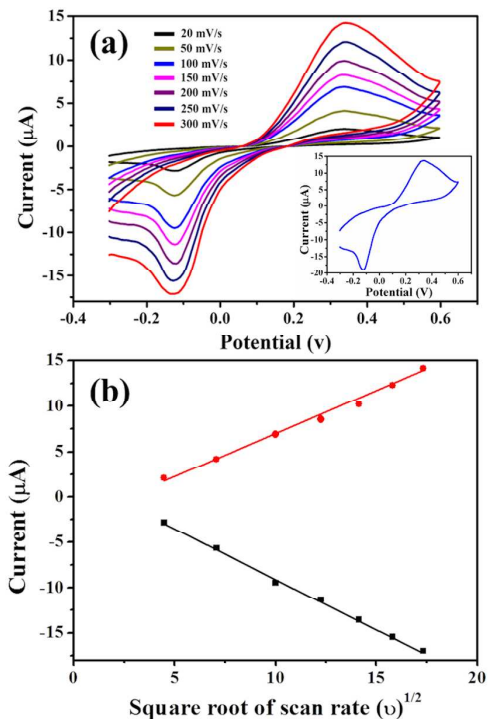
Fig. 5 (a) CV of Ag/α-Fe$_2$O$_3$/GOx/Nafion electrode in 0.1M PBS (pH 7.0) containing 0.2 mM glucose at different scan rates; (b) Linear relationship of Ip and square root of scan rate (υ) at modified electrode. Inset in (a) shows the CV curve in the presence of 0.1 mM H$_2$O$_2$ in PBS at scan rate of 100 mV/s.

GOx and H$_2$O$_2$ reduction, respectively. The sharp peaks were observed from the CV curves of Ag/α-Fe$_2$O$_3$/GOx/Nafion electrode for 0.2, 0.5 and 1.0 mM glucose, which relates to the oxidation of glucose by GOx. We also measured CV in the presence of only H$_2$O$_2$ (inset of Fig. 5(a)). This further confirms that the redox peaks appeared at +0.33 V and -0.12 V are due to the H$_2$O$_2$ and H$_2$O$_2$ reduction, respectively. Fig. 5(a) demonstrates the CV curves for the modified Ag/α-Fe$_2$O$_3$/GOx/Nafion electrode in presence of 0.2 mM glucose measured at different scan rates, i.e. 20, 50, 100, 150, 200, 250 and 300 mV/s, respectively. It is worth noting that the linear relationship of i$_p$ *vs.* υ$^{1/2}$ derived from the CV shows a near-perfect scaling of the steady-state current. This confirms that the reaction is occurring in a diffusion-controlled manner for oxidation and reduction of H$_2$O$_2$. The observed curve for the oxidation and reduction peak current as a function of the square root of the scan rates in the range of 20-300 mV is shown in Fig. 5(b) with R^2 of 0.9916 for I_{pa} and 0.9983 for I_{pc}, respectively).

A typical steady-state amperometric response of a modified Ag/α-Fe$_2$O$_3$/GOx/Nafion electrode biosensor is shown Fig. 6(a and b), with the successive addition of glucose in 0.1 M PBS (pH = 7.0) at an applied potential of +0.33 V under stirring condition. A rapid and sensitive response to each injection of glucose was obtained with response time of less than 2s for the enzyme electrode to reach 98% steady state current. It is also clearly seen from the graph that the response current increases as the concentration of glucose increases and saturated at high concentration of glucose, which suggests the saturation of active sites of the enzymes at those glucose levels. Fig. 6(c) exhibits a calibration curve for the response current *vs.* glucose
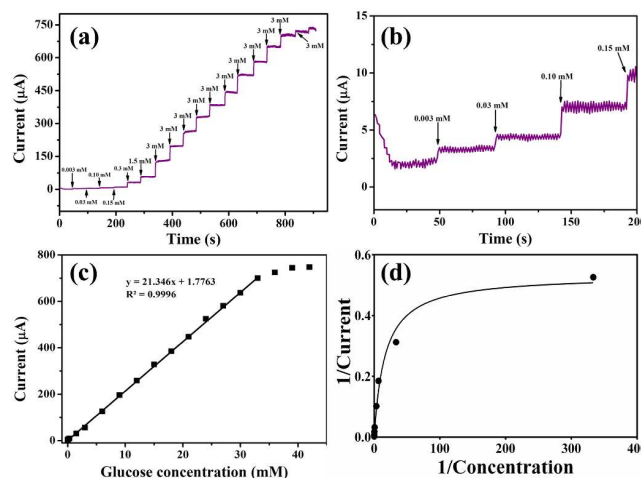
Fig. 6 (a) The amperometric response of Ag/α-Fe$_2$O$_3$/GOx/Nafion electrode to different concentrations of glucose at +0.33 V in 0.1M PBS (pH 7.0); (b) Amperometric response in the range of 0.003 - 0.15 mM glucose concentration; (c) Calibration curve of the Ag/α-Fe$_2$O$_3$/GOx/Nafion electrode with successive additions of glucose; (d) The Lineweaver-Burk plot of 1/i *vs.* 1/C.

concentration of the fabricated glucose biosensor. From the calibration curve, the biosensor exhibited a linear range of 0.003 - 33.0 mM (R^2 = 0.9996), sensitivity of 85.384 µA/mMcm^{2}and detection limit of 1 µM (S/N = 3). The high sensitivity of the enzyme electrode can be attributed to the excellent adsorption ability, high electro-catalytic activity and good biocompatibility of the spruce branched α-Fe$_2$O$_3$ nanostructures.[36-39] The estimated sensitivity of the fabricated biosensor is relatively higher and detection limit is lower than previously reported glucose biosensors based on other nanomaterials modified electrodes (Table 1).[40-49] The apparent K_m^{app}, which gives an indication of the enzyme-substrate kinetics can be calculated from the Lineweaver-Burk equation $1/i = ((K_m^{app})/i_{max}) (1/C) + (1/i_{max})$, where i is the current, i$_{max}$ is the maximum current measured under saturated substrate conditions, and C is the glucose concentration (Fig. 6(d)). According to the Lineweaver-Burk plot, the K_m^{app} is calculated to be 16.52 mM implying that the modified Ag/α-Fe$_2$O$_3$/GOx/Nafion electrode recycles reduced enzyme quite efficiently leading to a wide linear dynamic range.
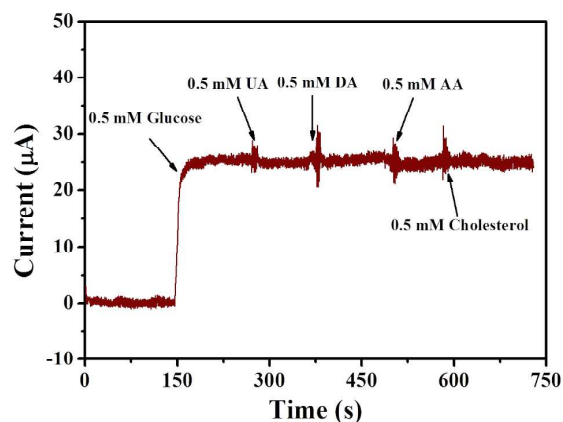
Fig. 7 Effect of interfering species on the biosensor response with subsequent addition of 0.5 mM of glucose, uric acid (UA), dopamine (DA), ascorbic acid (AA), and cholesterol, respectively in the 0.1M PBS (pH 7.0).

Table 1: Comparison of amperometric glucose biosensor performance constructed based on different modified electrode materials.

Electrode Materials	Sensitivity ($\mu AmM^{-1}cm^{-2}$)	K_m^{app}/mM	Detection Limit/μM	Response time/s	Ref.
Spruce branched α-Fe$_2$O$_3$ nanostructures	85.384	16.52	1.0	<2	This work*
ZnO nanocombs	15.33	2.19	20	<10	40
ZnO nanorods	23.1	2.9	10	<5	41
Titania sol-gel membrane	7.2	6.34	70	<6	42
Cerium Oxide	0.00287	13.55	12.0	<5	43
Nanoporous ZrO$_2$/chitosan film	0.028	3.14	10	<10	44
Cadmium Sulphide	7.0	-	50	-	45
Poly(o-aminophenol) film/poly-pyrrole-Ptnano-composite	9.9	23.9	0.45	~7	46
Multilayer films of chitosan, gold nanoparticles	0.555	10.5	7	<8	47
Au NPs-mesoporous silica nanocomposite	2.95	-	45	<12	48

*All the measurements were made in an air-saturated buffer (0.1M PBS).

Due to the unique morphology of spruce branched α-Fe$_2$O$_3$ nanostructures, the fabricated biosensor exhibits better performance. Where, a high specific surface area of α-Fe$_2$O$_3$ nanostructures leads to GOx loading with large quantity and also works as a favorable microenvironment to keep the enzyme in active form. Moreover, the high conductivity of α-Fe$_2$O$_3$ provides a high electron communication feature, which results in higher-sensitivity and lower detection limit from our fabricated Ag/α-Fe$_2$O$_3$/GOx/Nafion electrode.

3.3. Selectivity test

The anti-interference ability of the biosensor is investigated, as it is well known that some electroactive species in serum may influence the performance of a biosensor. Therefore, the 0.5 mM of each electro-active species such as uric acid, dopamine, ascorbic acid and cholesterol were added respectively in the 0.1M PBS (pH 7.0). The influences of the above species on the detection of glucose at the α-Fe$_2$O$_3$ nanostructures modified electrodes are shown in Fig.7. The observation clearly exhibited

that the interfering species do not have any obvious effect on the biosensor performance. It suggests that the fabricated electrodes are favorable for the selective determination of glucose in the presence of interfering species.

3.4. Reproducibility and storage stability test

To examine the reproducibility and long-term storage stability, we fabricated five different bioelectrodes in similar fabrication conditions. Their responses were recorded (Fig. 8(a)) which exhibited that the fabricated biosensors are reproducible for glucose detection. For repeatability, the response for the Ag/α-Fe$_2$O$_3$/GOx/Nafion biosensor was examined with respect to the storage time. After each experiment, the sensor was washed with the buffer solution and stored in a 0.1 M PBS at 4.0 ^{o}C and no obvious decrease in currents for the direct electron transfer and the response to GOx was observed (Fig. 8(b)). The long-term storage stability of the sensor was tested for 8 weeks. The sensitivity retained ~95% of initial sensitivity up to 5 weeks and after that the response of the fabricated sensor gradually decreases.

3.5. Real sample analysis

The workability of the fabricated glucose biosensors was checked in the known concentration of glucose in human serum samples (4.89 mM; Sigma-Aldrich, H4522) after dilution (sample 1-2) in 0.1 M PBS. Each sample was analyzed three times to calculate their relative standard deviation (RSD) during measurements. Where, RSD is estimated by dividing the standard deviation by the average; then multiply by 100 to be expressed as a percentage. The obtained data is shown in Table 2. A lower percentage of RSD indicates a lower variability in the data set. Further, the accuracy and precision of the sensor was examined by standard addition of pure glucose (5.0 mM) to the known certified concentration of glucose in human serum samples (sample 1-2).[49] The concentrations of the standard additions were determined after deducting the known certified concentration of glucose in human serum sample from the total measured value (after adding pure glucose). Then, the determined concentrations of the standard additions and their percent recovery measured by our sensor were compared to the standard additions (Table 2). The data are in good agreement with the known concentration of glucose, demonstrating that our fabricated glucose biosensor studied in this work exhibit good repeatability and reliability.
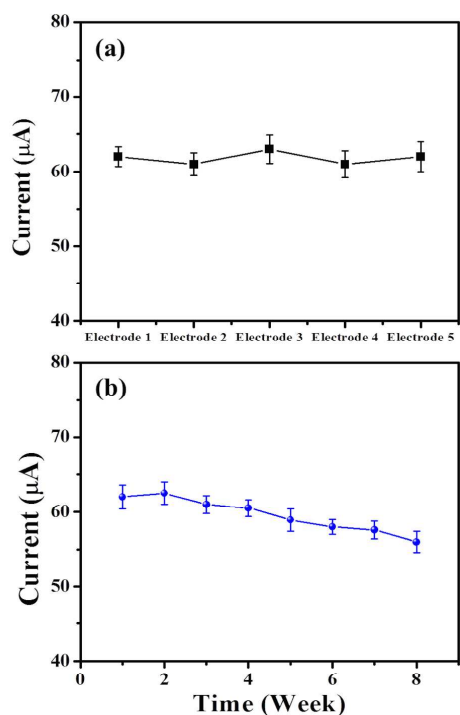
Fig. 8 (a) Reproducibility and (b) storage stabilities study of the fabricated glucose biosensors in 1.0 mM glucose.

Table 2 Determination of glucose in human serum samples.

Sample	Certified conc. of serum sample	Determined conc. of serum sample	RSD (%) (n=3)	Standard addition of pure glucose	Determined conc. for standard addition	RSD (%) (n=3)	Recovery of added standard (%)
1	1.22 mM	1.21 mM	0.9	5.0 mM	4.85 mM	2.1	97
2	2.45 mM	2.43 mM	1.6	5.0 mM	4.70 mM	1.9	94
4	4.89 mM	4.91 mM	1.3	5.0 mM	4.90 mM	3.8	98

4. Conclusions

In summary, highly-sensitive and selective amperometric glucose biosensor based on spruce branched α-Fe$_2$O$_3$ nanostructures are fabricated. The fabricated glucose biosensor exhibited a very high and reproducible sensitivity of 85.384 μAmM^{-1}cm^{-2} with a detection limit of 1μM. Moreover, the fabricated biosensor exhibited an excellent anti-interference ability against various electroactive species. These results demonstrate that α-Fe$_2$O$_3$ nanostructures are promising scaffold for the fabrication of highly-sensitive and selective amperometric biosensors.

Acknowledgements

Notes and references

[a] Promising Centre for Sensors and Electronic Devices (PCSED), Najran University, P.O. Box 1988, Najran-11001, Kingdom of Saudi Arabia. Tel: +966-534574597; E. mail: ahmadumar786@gmail.com
[b] Department of Chemistry, Faculty of Science and Arts, Najran University, P.O. Box 1988, Najran-11001, Kingdom of Saudi Arabia
[c] School of Semiconductor and Chemical Engineering, and Nanomaterials Processing Research Center, Chonbuk National University, 567 Baekjedaero, Deokjin-gu, Jeonju 561-756, Republic of Korea
†Authors contributed equally to this work.

1 The Diabetes Control and Complications Trial Research Group, *N. Engl. J. Med.,* 1993, **329**, 977.
2 WHO (2009) Fact sheet No. 312 in World Health Organization.
3 Y. Wang, H. Xu, J. Zhang and G. Li, *Sensors*, 2008, **8**, 2043.
4 M. Morikawa, N. Kimizuka, M. Yoshihara and T. Endo, Chem. Eur. J., 2002, 8, 5580.
5 Y. Miwa, M. Nishizawa, T. Matsue and I. Uchida, *Bull. Chem. Soc. Jp.,* 1994,**67**, 2864.
6 S. Mansouri and J. S. Schultz, *Nat. Biotech.,* 1984,**2**, 885.
7 J. C. Pickup, F. Hussain, N. D. Evans, O. J. Rolinski and D. J. S. Birch, *Biosens. Bioelectron.,* 2005,**20**, 2555.
8 S. Liu, B. Yu and T. Zhang,*Electrochim. Acta,* 2013,**102**, 104.
9 S. Liu, J. Tian, L. Wang, X. Qin, Y. Zhang, Y. Luo, A. M. Asiri, A. O. Al-Youbi and X. Sun, *Catal. Sci. Technol.,* 2012,**2**, 813.
10 S. Liu, J. Tian,L. Wang, Y. Luo, W. Lu and X. Sun, *Biosens. Bioelectron.,* 2011,**26**, 4491.
11 X. Y. Liu, X. D. Zeng, N. N. Mai, Y. Liu, B. Kong, Y. H. Li, W. Z. Wei and S. L. Luo, *Biosens. Bioelectron.,* 2010,**25**, 2675.
12 J. Jung and S. Lim, *Appl. Surface Sci.,* 2013,**265**, 24.
13 H. Wang, H. Ohnuki, H. Endo and M. Izumi, Sens. Actuators, 2012,**168**, 249.
14 L. Jin, X. Gao, H. Chen, L. Wang, Q. Wu, Z. Chen and X. Lin, J. Electrochem. Soc., 2013,**160**, H6.
15 J. Du, Y. Wang, X. Zhou, Z. Xue, X. Liu, K. Sun and X. Lu, J. Phys. Chem. C, 2010, **114**, 14786.
16 C. X. Guo and C. M. Li, *Phys. Chem. Chem. Phys.,* 2010,**12**, 12153.
17 J. Zang, C. M. Li, X. Cui, J. Wang, X. Sun, H. Dong and C. Q. Sun, *Electroanalysis,* 2007,**19**, 1008.
18 K. Ogata, H. Dobashi, K. Koike, S. Sasa, M. Inoue and M. Yano, *Physica E,* 2010,**42**, 2880.
19 R. Ahmad, N. Tripathy, J. H. Kim and Y.-B. Hahn, *Sens. Actuators B: Chem.,* 2012,**174**, 195.
20 R. Ahmad, N. Tripathy and Y.-B. Hahn, *Sens. Actuators B: Chem.,* 2012,**169**, 382.
21 M. Viticoli, A. Curulli, A. Cusma, S. Kaciulis, S. Nunziante, L. Pandolfi, F. Valentini and G. Padeletti, *Mater. Sci. Eng. C*, 2006,**26**, 947.
22 S. P. Singh, S. K. Arya, P. Pandey, B. D. Malhotra, S. Saha, K. Sreenivas and V. Gupta, *Appl. Phys. Lett.,* 2007,**91**, 063901.
23 Z. Yang. Y. Tang, J. Li, Y. Zhang and X. Hu, *Biosens. Bioelectron.,* 2014,**54**, 528.
24 C. W. Liao, J. C. Chou, T. P. Sun, S. K. Hsiung and J. H. Hsieh, *IEEE Trans. Biomed. Eng.,* 2006,**53**, 1401.
25 Y.-B. Hahn, R. Ahmad and N. Tripathy, *Chem. Commun.,* 2012,**48**, 10369.
26 Z. Yang, X. Huang, R. Zhang, J. Li, Q. Xu and X. Hu, *Electrochim. Acta,* 2012,**70**, 325.
27 S. Saha, S. K. Arya, S. P. Singh, K. Sreenivas, B. D. Malhotra and V. Gupta, *Biosens. Bioelectron.,* 2009,**24**, 2040.
28 V. Gupta, *Thin Solid Films,* 2010,**519**, 1141.
29 Z. Yang, Y. Ren, Y. Zhang, J. Li, H. Li, X. Huang, X. Hu and Q. Xu, *Biosens. Bioelectron.,* 2011,**26**, 4337.
30 J. Hrbac, V. Halouzka, R. Zboril, K. Papadopoulos and T. Triantis, *Electroanalysis,* 2007,**19**, 1850.
31 A. Kaushik, R. Khan, P. R. Solanki, P. Pandey, J. Alam, S. Ahmad and B. D. Malhotra, *Sens. Actuators B: Chem.,* 2009,**138**, 572.
32 S. F. Wang and Y. M. Tan, *Anal. Biochem.,* 2007,**387**, 703.
33 M. Abaker, A. Umar, S. Baskoutas, G. N. Dar, S. A. Zaidi, S. A. Al-Sayari, A. Al-Hajry, S. H. Kim and S. W. Hwang, *J. Physics D: Applied Physics,* 2011,**44**, 425401.
34 S. P. S. Porto and R. S. Krishnan, *J. Chem. Phys.,* 1967,**47**, 1009.
35 A. Kaushik, R. Khan, P.R. Solanki, P. Pandey, P. Alam, S. Ahmad and B.D. Malhotra, *Biosens. Bioelectron.,* 2008,**24**, 676.
36 K.J. Cash and H.A. Clark, *Trends in Molecul. Medicine,* 2010,**16**, 584.
37 T. Maiyalagan, J. Sundaramurthy, P. Suresh Kumar, P. Kannan, M. Opallo and S. Ramakrishna, *Analyst*, 2013,**138,** 1779.
38 S.-W. Cao, Y.-J. Zhu, M.-Y. Ma, L. Li and L. Zhang, *J. Phys. Chem. C*, 2008,**112**, 1851.
39 M. Ahmad, C. Pan, Z. Luo and J. Zhu, *J. Phys. Chem. C*, 2010,**114**, 9308.
40 J. X. Wang, X. W. Sun, A. Wei, Y. Lei, X. P. Cai, C. M. Li and Z. L. Dong, *Appl. Phys. Lett.,* 2006, **88**,233106.
41 A. Wei, X. W. Sun, J. X. Wang, Y. Lei, X. P. Cai, C. M Li, Z. L. Dong and W. Huang, *Appl. Phys. Lett.,* 2006,**89**, 123902.
42 J. Yu, S. Liu and H. Ju, *Biosens. Bioelectron.,* 2003,**19**, 401.
43 A. A. Ansari, P. R. Solanki and B. D. Malhotra, *Appl. Phys. Lett.,* 2008,**92**, 263901.
44 Y. Yang, H. Yang, M. Yang, Y. Liu, G. Shen and R. Q. Yu, *Anal. Chim. Acta,* 2004,**525**, 213.
45 Y. Huang, W. Zhang, H. Xiao and G. Li, *Biosens. Bioelectron.,* 2005,**21**, 817.
46 J. Li and X. Lin, *Biosens. Bioelectron.,* 2007,**22**, 2898.
47 B. Wu, S. Hou, F. Yin, J. Li, Z. Zhao, J. Huang and Q. Chen, *Biosens. Bioelectron.,* 2007,**22**, 838.
48 Y. Bai, H. Yang, W. Yang, Y. Li and C. Sun, *Sens. Actuators B: Chem.,* 2007,**124**, 179.
49 R. Ahmad, M. Vaseem, N. Tripathy and Y.-B. Hahn, *Anal. Chem.,* 2013,**85**, 10448.

New Journal of Chemistry Accepted Manuscript